

Fig. 3. Circuit diagram of the differential pair, T/H and output driver blocks. All MOSFETs have a drawn gate length of  $0.13\mu\text{m}$ .

range. This is realized by choosing a low noise broadband input stage and biasing the transistors in the data path at  $0.25\text{ mA}/\mu\text{m}$  for a good compromise between bandwidth, low-noise and high linearity.

A clock distribution network provides the differential clock signal to the T/H block. It consists of the same TIA-CS front-end as the data path, followed by three CML inverters. These stages operate in digital mode and are biased at  $0.15\text{ mA}/\mu\text{m}$  for maximum switching speed. The circuit is powered from a 1.8-V supply and consumes 270 mW. The T/H block and the clock distribution network consume 12 mA and 70 mA respectively, while the remaining 68 mA of current is drawn by the input and output blocks.

#### A. Transimpedance Amplifier (TIA)

Instead of using  $50\Omega$ -terminated differential pairs, this design employs a low noise TIA input stage (Fig. 2). A TIA provides simultaneous noise and signal matching without the need for  $50\Omega$  matching resistors. Noise matching is achieved by sizing the input transistors ( $Q_{1-2}$ ) to produce an optimum source impedance of  $50\Omega$  [11]. The input impedance is set by the feedback resistor  $R_F$ . Active PMOS loads ( $Q_{3-4}$ ) are used to increase the open loop gain and maximize the linearity of the TIA. At DC, transistors  $Q_1$  and  $Q_2$  are diode connected and thus the output of the TIA biases the transistors  $Q_{5-6}$  [12]. The input-referred noise power spectral density of the cascade of the TIA and the differential pair stages obtained from simulation and integrated up to 30 GHz is  $0.5\text{ mV}_{\text{rms}}$ .

#### B. Track and Hold Stage

Fig. 3 shows the schematic diagram of the T/H amplifier with a differential pair input and output driver. In track mode,  $\text{Clk}_P$  is high,  $Q_{SF}$  acts as a source follower and the output follows the input signal. In hold mode,  $\text{Clk}_N$  is high and the

tail current  $I_T$  flows through the loads of the differential pair,  $R_L$ . The value of  $R_L$  is chosen such that the voltage drop  $I_T R_L$  turns off transistor  $Q_{SF}$  and provides good isolation between the input and the output. The power supply voltage required by this design is dictated by  $I_{Diff} R_L + V_{GS-QSF} + V_{GS-QDRV}$ .

Taking advantage of the triple well option in this process, the bulk and source of  $Q_{SF}$  are shorted together to minimize  $V_{GS-QSF}$  and allow for a  $600\text{-mV}_{P-P}$  signal swing at the output of the source follower. Even though a 1.8-V supply is required, the voltage drop across individual transistors does not exceed 1.2 V. The hold capacitance,  $C_H = 250\text{ fF}$ , includes the parasitic capacitances at that node and a  $50\text{ fF}$  MIM capacitor. The value of  $C_{fth}$  is chosen to match  $C_{GS-QSF}$  and to cancel hold mode signal feedthrough.

#### C. Clock Distribution Network

The clock path converts a single-ended 30-GHz clock input to a differential signal with  $750\text{ mV}_{P-P}$  swing per side at the two switching pairs ( $Q_T$  and  $Q_H$ ) in the T/H block. The blocks in the clock path operate at 30 GHz, the highest operating frequency of this circuit. It consists of a TIA stage (identical to Fig. 2) followed by three CML inverters. The schematic of the final three CML inverting stages is shown in Fig. 4. In order to ensure that every stage is fully switched, the gain of the inverters in the clock path is designed to exceed  $\sqrt{2}$ .

### III. FABRICATION AND TESTING

The chip was fabricated in a  $0.13\mu\text{m}$  CMOS technology. The chip area is  $1\text{ mm}^2$  and the die photo is shown in Fig. 5. All measurements were conducted on-wafer with single-ended input and clock signal.

The simulated and measured S-parameters are shown in Fig. 7. The input and output return loss are better than  $-10\text{ dB}$

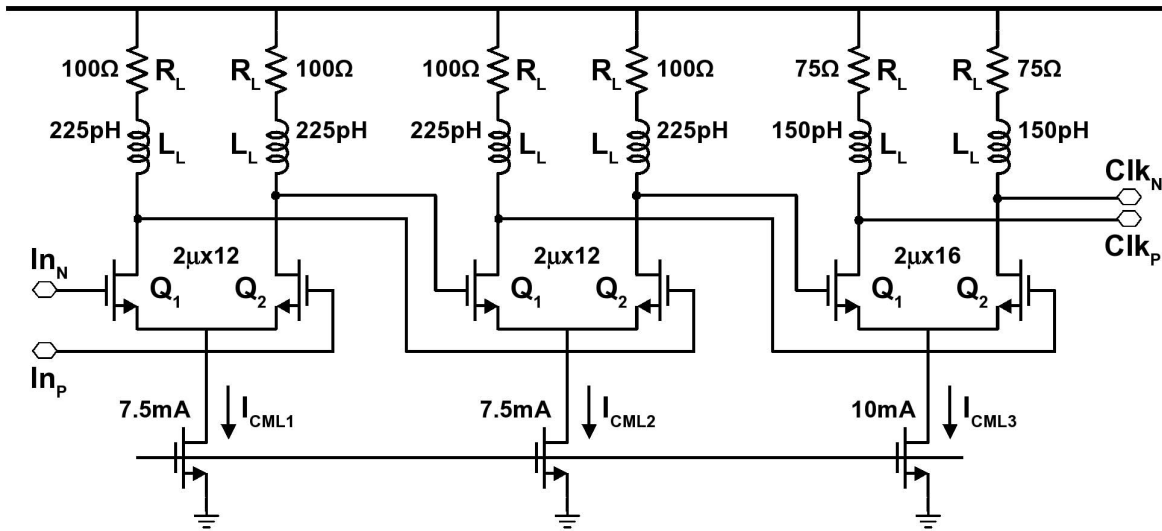


Fig. 4. Circuit diagram of the final three CML inverting stages of the clock path. All MOSFETs have a drawn gate length of  $0.13\mu\text{m}$ .

up to 35 GHz.  $S_{21}$  has a bandwidth of 7 GHz when the circuit is operated in track mode. Since the front end of the data and clock paths are identical, the input return loss of the data path is also representative of the clock input return loss which is less than  $-15$  dB from 22 GHz to 32 GHz.

Fig. 6 illustrates the two single ended outputs for a  $-12$  dBm, 5-GHz input signal sampled at 30 GHz. Signal droop rate was measured at low clock frequencies to be less than  $10$  mV/ns. For a 30-GHz sampling frequency, this translates to a droop of only  $0.2$  mV per held value.

The input and output compression points of the circuit were measured from 1 GHz to 14 GHz in 1-GHz steps and are illustrated in Fig. 8. Fig. 9 shows the measured IIP3 and OIP3 as a function of frequency. The OIP3 plot indicates a circuit bandwidth of 7 GHz, in close agreement with the  $S_{21}$  measurement. Simulations show that the hold node is the bandwidth-limiting node of this circuit. The measured SFDR

and THD are illustrated in Fig. 10. SFDR is calculated from the measured spectra and simulated noise floor integrated over a 30-GHz bandwidth, (evaluated to be  $-53$  dBm). The THA has an SFDR of 40 dB at 1 GHz with 7 GHz of bandwidth.

#### IV. CONCLUSIONS

A 30-GS/sec CMOS THA was designed and fabricated in a  $0.13\text{-}\mu\text{m}$  CMOS process. Following a systematic design procedure, and combining a low noise front-end with signal feedthrough cancellation and power supply voltage reduction techniques, has yielded the highest sampling frequency THA in CMOS. With a THD of better than  $-29$  dB and 7 GHz of bandwidth, this THA is a potential contender for the front end of a 30 GS/sec flash ADC. Such an ADC can be used in over-sampling DSP based receivers for 10 Gbps applications.

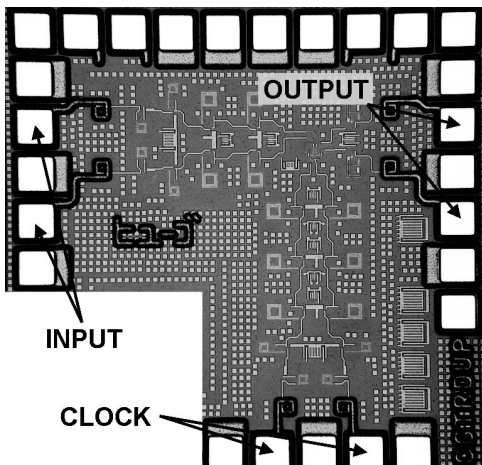


Fig. 5. Die photo of the fabricated THA

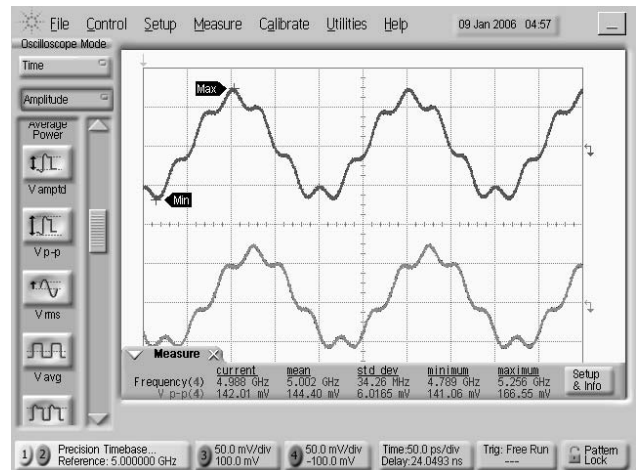


Fig. 6. Single ended outputs of a 5-GHz sinusoid sampled at 30 GHz.

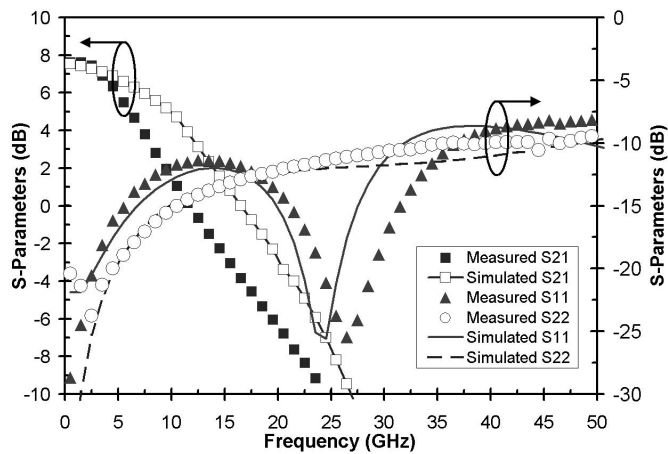


Fig. 7. Simulated and measured single-ended THA input return loss ( $S_{11}$ ), output return loss ( $S_{22}$ ) and transmission ( $S_{21}$ ).

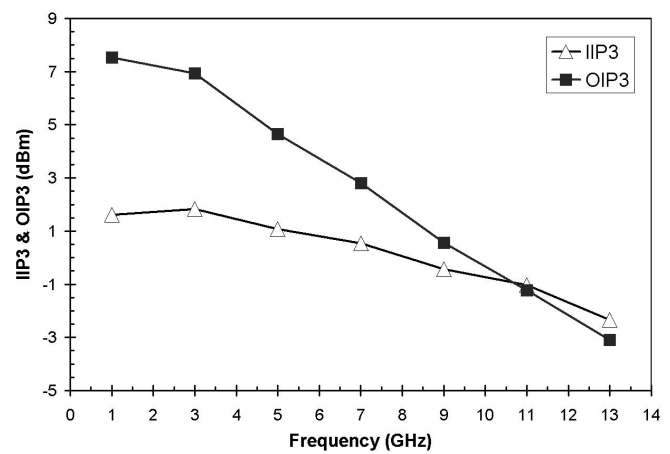


Fig. 9. Measured IIP3 and OIP3 versus input frequency with 30-GHz clock frequency.

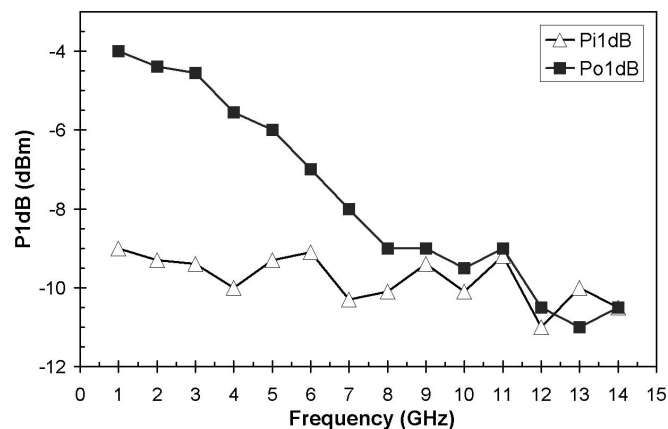


Fig. 8. Measured  $P_{i1dB}$  and  $P_{o1dB}$  versus input frequency with 30-GHz clock frequency.

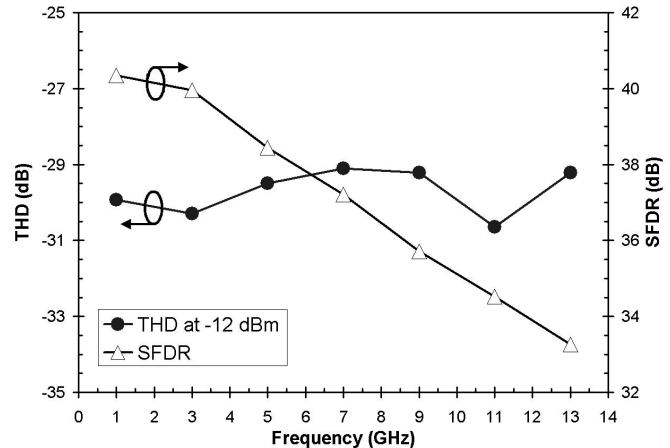


Fig. 10. Measured SFDR and THD versus frequency with 30-GHz clock frequency. The measured THD is shown for signals with -12 dBm input power.

#### ACKNOWLEDGMENT

We would like to acknowledge CMC for fabrication and providing the CAD tools, NSERC for their financial support, OIT and CFI for equipment grants and ECTI for providing the network analyzer.

#### REFERENCES

- [1] A. Garg, A. C. Carusone, and S. P. Voinigescu, "A 1-tap 40-Gbps look-ahead decision feedback equalizer in  $0.18\mu\text{m}$  SiGe BiCMOS technology," in *CSICS, Proceedings of the IEEE*, Oct. 2005, pp. 37–40.
- [2] A. Hazneci and S. P. Voinigescu, "49-Gb/s, 7-tap transversal filter in  $0.18\mu\text{m}$  SiGe BiCMOS for backplane equalization," in *CSICS, Proceedings of the IEEE*, Oct. 2004, pp. 101–104.
- [3] P. Schvan, D. Pollex, S. Wang, C. Falt, and N. B. Hamida, "A 22GS/s 5b ADC in  $0.13\mu\text{m}$  SiGe BiCMOS," in *Solid-State Circuits Conference, IEEE International, Digest of Technical Papers*, Feb. 2006, pp. 572–573.
- [4] P. Vorenkamp and J. Verdaasdonk, "Fully Bipolar, 120-MSample/s 10-b track-and-hold circuit," *IEEE J. Solid-State Circuits*, pp. 988–992, Sept. 1992.
- [5] S. Shahramian, A. C. Carusone, and S. Voinigescu, "A 40-GSamples/Sec Track & Hold Amplifier in  $0.18\mu\text{m}$  SiGe BiCMOS technology," in *CSICS, Proceedings of the IEEE*, Oct. 2005, pp. 101–104.

- [6] T. Sato, S. Takagi, N. Fujii, Y. Hashimoto, K. Sakata, and H. Okada, "4-Gb/s Track and Hold Circuit using Parasitic Capacitance Canceller," in *ESSCIRC, Proceeding of the IEEE*, Sept. 2004, pp. 347–350.
- [7] A. Boni, A. Pierazzi, and C. Morandi, "A 10-b 185-MS/s Track-and-Hold in  $0.35\text{-}\mu\text{m}$  CMOS," *IEEE J. Solid-State Circuits*, pp. 195–203, Feb. 2001.
- [8] N. Tchamov, M. Velichkov, A. Keranen, and V. Stoyanov, "Differentially pre-compensated GHz-range low-voltage track-and-hold," in *Electronic Letters*, Jan. 2003, p. 180.
- [9] Y. Lu, W. Kuo, X. Li, R. Krithivasan, J. Cressler, Y. Borokhovych, H. Gustat, B. Tillack, and B. Heinemann, "An 8-bit, 12 GSamples/sec SiGe track-and-hold amplifier," in *BCTM, Proceedings of the IEEE*, Oct. 2005, pp. 148–151.
- [10] J. Lee, A. Leven, J. Weiner, Y. Baeyens, Y. Yang, W. Sung, J. Frachoviak, R. Kopf, and Y.-K. Chen, "6-b 12-GSamples/S track-and-hold amplifier in InP DHBT Technology," *IEEE J. Solid-State Circuits*, pp. 1533–1539, Sept. 2003.
- [11] S. Voinigescu, T. Dickson, T. Chalvatzis, A. Hazneci, E. Laskinand, R. Beerkens, and I. Khalid, "Algorithmic Design Methodologies and Design Porting of Wireline Transceiver IC Building Blocks Between Technology Nodes," in *CICC, Proceedings of the IEEE*, Sept. 2005, pp. 110–117.
- [12] F. Pera and S. Voinigescu, "An SOI CMOS, High Gain and Low Noise Transimpedance-Limiting Amplifier for 10Gb/s Applications," in *Accepted for presentation at RFIc*, June 2006.